Supporting Information

Novel amine-functionalized Mg-MOF CO_2 adsorbents with a bi-functional adsorption-screening

Xiaotong Jiang [a], Liju Bai [a], Shuai Wang [a], Yimin Deng [a], Jan Baeyens [b], Martin Schiemann [c], Helei Liu [a*]

[a] Joint International Research Laboratory of Carbon Neutrality System and Engineering Management, Beijing Laboratory for System Engineering of Carbon Neutrality, School of Chemistry and Chemical Engineering, Beijing Institute of Technology, Beijing, 102488, China

[b] KULeuven, Department of Chemical Engineering, Process and Environmental Technology Lab., 2860 Sint-Katelijne-Waver, Belgium

[c] Ruhr University Bochum, Faculty of Mechanical Engineering, Department of Energy Plant Technology, Universitätsstraße 150, 44801, Bochum, Germany

*Corresponding author: Prof. Helei Liu: hl_liu@bit.edu.cn

Experimental Procedures

1. Conditions for synthesizing Mg-MOFs and Amine-Mg-MOFs

Preparation of Mg-MOF-74-a by water at room temperature. Performed according to the literature synthesis method[1]. The synthesized yellow powder adsorbent was noted as Mg-MOF-a.

Preparation of Mg-MOF-74s by solvothermal synthesis. The raw metal material of magnesium nitrate (0.192 g, 0.75 mmol) was dissolved in 16.5mL methanol solution to form a metal ionic liquid. Subsequently, (0.059 g, 0.30 mmol) H_4DOBDC ligand dissolved in 13.5 mL DMF to form a solution of ligand compounds. The two solutions were mixed and placed in a reactor to be reacted for 12 h at 130 ℃, 150 ℃, 180 ℃. The synthesized yellow powder adsorbent was noted as Mg-MOF-b.

Magnesium acetate (0.107 g, 0.75 mmol) was dissolved in 16.5 mL methanol solution to form a metal ionic liquid. Thereafter, H_4DOBDC (0.059 g, 0.30 mmol) ligand was dissolved in 13.5 mL DMF to form a solution of ligand compounds. The two solutions were mixed and placed in a reactor for 12 h at 180 ℃. The synthesized yellow powder adsorbent was noted as Mg-MOF-c.

Finally, magnesium acetate (0.107 g, 0.75 mmol) was dissolved in 16.5 mL methanol solution to form a metal ionic liquid. H_4DOBDC (0.059 g, 0.30 mmol) ligand was dissolved in 13.5 mL DMF to form a solution of ligand compounds. Proton solvent deionized water was then provided after mixing the methanol/DMF metal salt and ligand compounds, adding 1 mL,1.5 mL,2 mL deionized water of the morphology and performance control additives, stirring achieved an evenly mixing to form a homogeneous phase. The solution was reacted for 12 h at 180 ℃. After the reactions, the suspension was centrifuged and washed twice with 20 mL DMF. The centrifuged solid was immersed in methanol for 72 h, and the solvent was replaced with fresh solvent every 24 h. Mg-MOF was placed in a vacuum oven at 80 ℃ and -0.1 MPa for 30 min to remove the methanol solvent, and the yellow solid powder adsorbent was finally obtained. The synthesized adsorbent was noted as Mg-MOF-e-g.

Preparation of amine-b/b'-Mg-MOF. Mg-MOF-d adsorbent was placed in a high-temperature

vacuum oven at 250 ℃, and the methanol solvent was removed for 5 h to obtain the Mg-MOF-d substrate material exposed to OMS. For 0.30 g of the activated substrate material, put 3,6-di-4-pyridyl-1,2,4,5-tetrazine(amine-b) molecule with grafting amount of 0.033 g (as MOF-amine-b) and 0.0001 g (as MOF-amine-b') together in the laboratory glass container, and then put both of them in the laboratory glass vials. The vial was submitted to a high-temperature vacuum drying oven at -0.1 MPa, and 250 °C. The solid amine molecules were sublimated to the vapor state under negative pressure, so that the solid amine molecules were fully contacted with the MOFs powders by vapor phase deposition, and the grafting time was controlled to be 2 h, to obtain the amine-modified solid adsorbent materials. To avoid solvent impurities retained in the pores during exposure to air and amine vapors attached to the adsorbent surface, the pre-treatment condition before adsorption was controlled at 120 °C for 1 h.

2. Calculations

Ideal Adsorbed Solution Theory (IAST) selectivity.

The calculation process was carried out using the pyGAPS program[2]. Calculate the adsorption conditions for a real flue gas mixture of 85% N_2 and 15% CO_2 partial pressure. The CO_2 adsorption isotherms were calculated using the Dual-Site Langmuir adsorption model[3] and the N_2 adsorption isotherms were calculated using the Langmuir model[4].

3. Theoretical calculations.

Periodic Grand canonical Monte Carlo (GCMC) calculations were performed to study the CO_2 adsorption density of CO_2 in Mg-MOFs synthesized in different conditions. The cell model of Mg-MOF-74 was obtained from The Cambridge Crystallographic Data Center (CCDC, ID 1863524)[5]. The OMS of the original MOF-74 crystal file was occupied by water molecules, periodic GCMC calculations were performed using the Material Studio (MS). Firstly, the single crystals of MOF-74 were subjected to 2×2×6 cell expansion to draw three supercells representing flower-like MOFs long pore structure, adherent MOFs pore structure and independent MOFs pore structure, relatively. The CO_2 and Mg-MOF-74 molecules optimized to be constructed by the AC module in the MS software were calculated and solved for the electric charge, and the dynamics under the classical

mechanical theory was employed to Forcite module under classical mechanics theory to select the COPASS II high-precision force field[6] for the charge calculation, and obtain the charge of C atoms 0.8 e and O atoms -0.4 e in CO_2, the charge of Mg atoms 1.876 e, O 0 e, H -0.255 e in Mg-MOF-74. Later, the physical adsorption density of CO_2 is calculated by the GCMC method with the Sorption module with setup of 1×10^6 equilibrium steps, sample step of 1×10^7, simulated temperature of 273 K, CO_2 pressure of 101.32 kPa, and an accuracy of Medium to obtain the three kinds of physical adsorption densities of Mg-MOF-74.

Periodic density functional theory (DFT) calculations. In the electronic scale for a high-precision ab initio density functional theory method, using the Castep calculation module in the Material Studio software, choose the LDA/CA-PZ[7] local exchange-correlation functional for optimization, the optimization parameters are set as follows: truncation energy cut off 310.0 eV, Brillouin zone k- point 1×1×1, and the total electron self-consistency of each atom converges to within 1×10^{-5} eV to obtain the lowest energy of the system.

Pore size calculations were performed to study the separation gas behavior of CO_2 and N_2 in amines-Mg-MOFs synthesized in systems modified with different amines. The geometrically optimized four amine structure-modified MOFs were imported into Zeo++ software[8, 9], and molecular probes were employed to investigate the structure and topology of the internal void space of the materials were analyzed based on geometry, and the three parameters of global cavity diameter (GCD), pore limiting diameter (PLD), and largest cavity diameter (LCD) were obtained in the calculation of the pore size. For the adsorption-screening bi-functional materials screening system in our work, the pore size of PLD is between the molecular dynamic diameters of CO_2 and N_2, 0.33-0.36 nm.

4. Results and Discussion.

4.1 Synthetic modulation of Mg-MOF-74 materials.

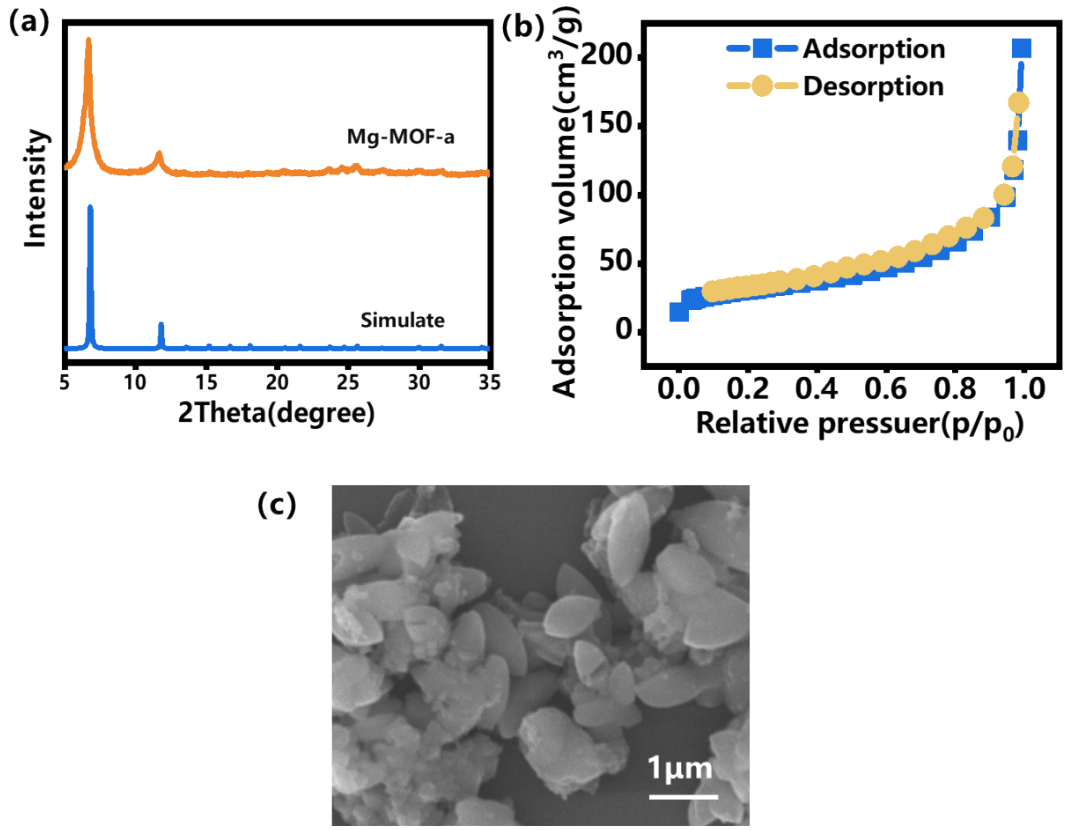

Figure S1. (a) XRD patterns, (b) Specific surface area and (c) SEM of water-based Mg-MOF-a crystal.

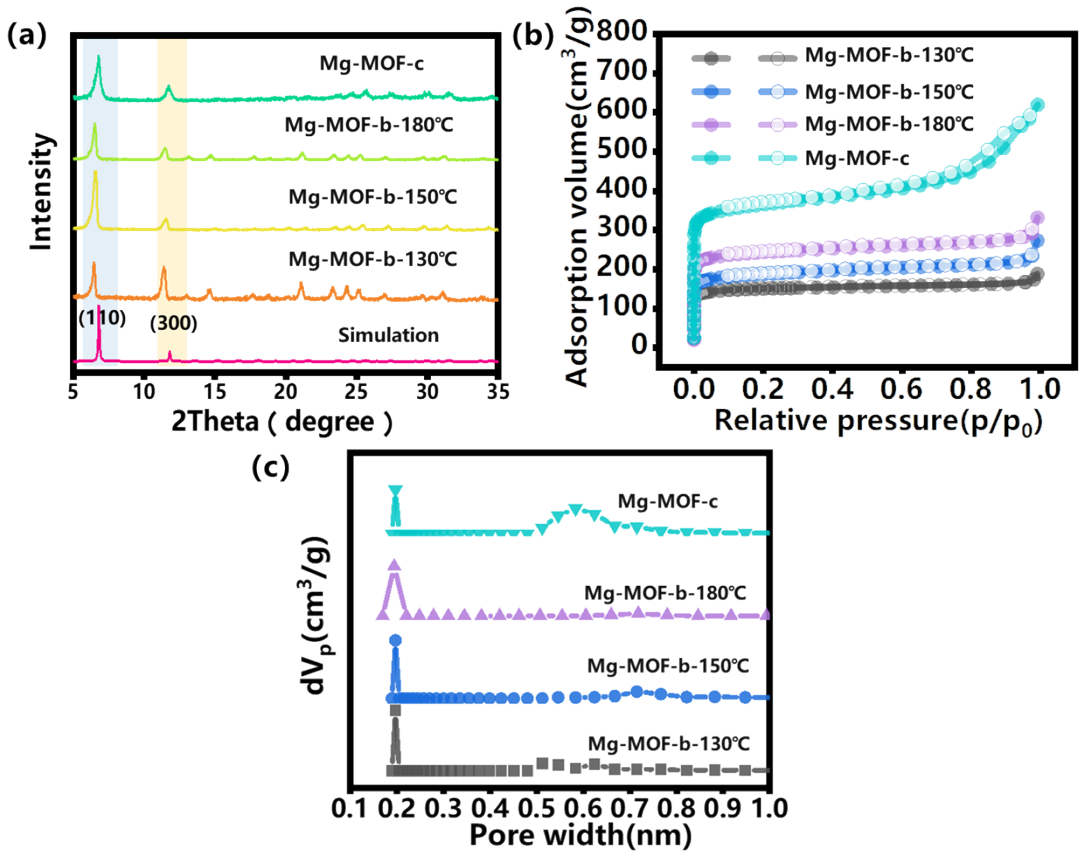

Figure S2. (a) XRD patterns, (b) Specific surface area and (c) Pore volume of Mg-MOF-b crystals at 130 ℃, 150 ℃, 180 ℃ and Mg-MOF-c, respectively.

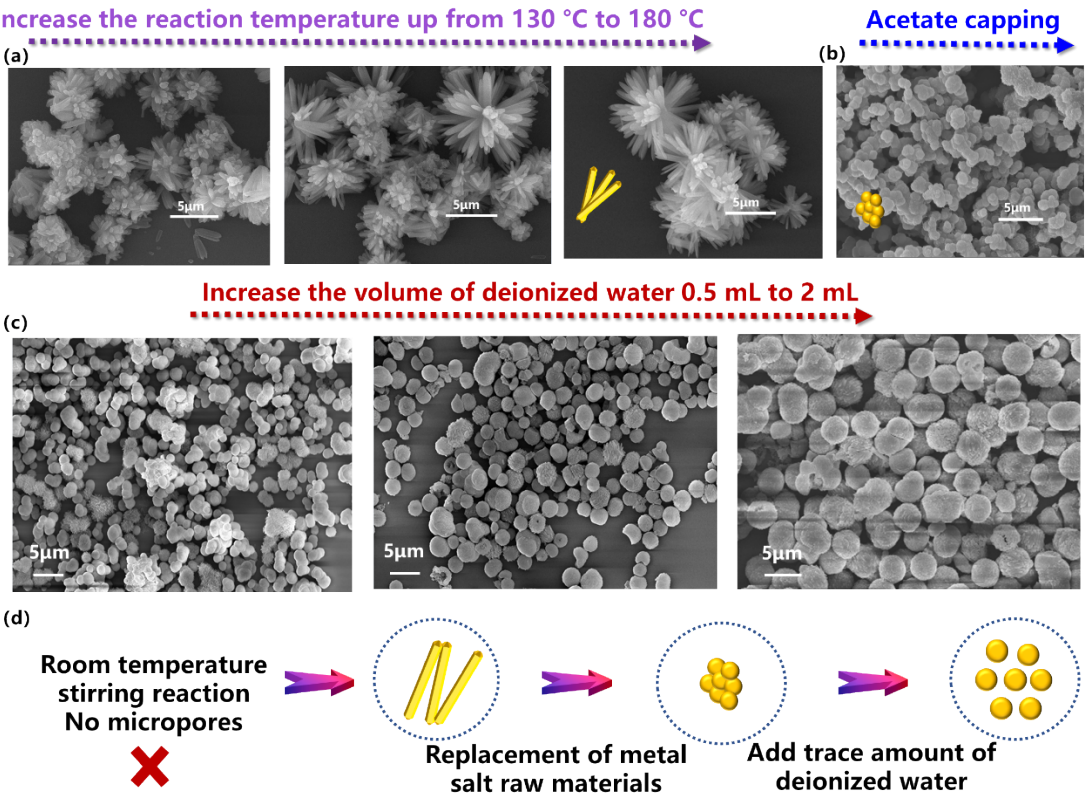

Figure S3. (a) SEM image of Mg-MOFs crystals, Mg-MOF-b crystals at 130 ℃, 150 ℃, 180 ℃ and Mg-MOF-c, respectively. (b) SEM images of Mg-MOF-c using magnesium acetate as synthetic raw metal. (c) SEM images of Mg-MOF-e synthesized with 1 mL deionized water, Mg-MOF-f synthesized with 1.5 mL deionized water and Mg-MOF-g synthesized with 2 mL deionized water, respectively. (d) Schematics of Mg-MOF synthesis regulation.

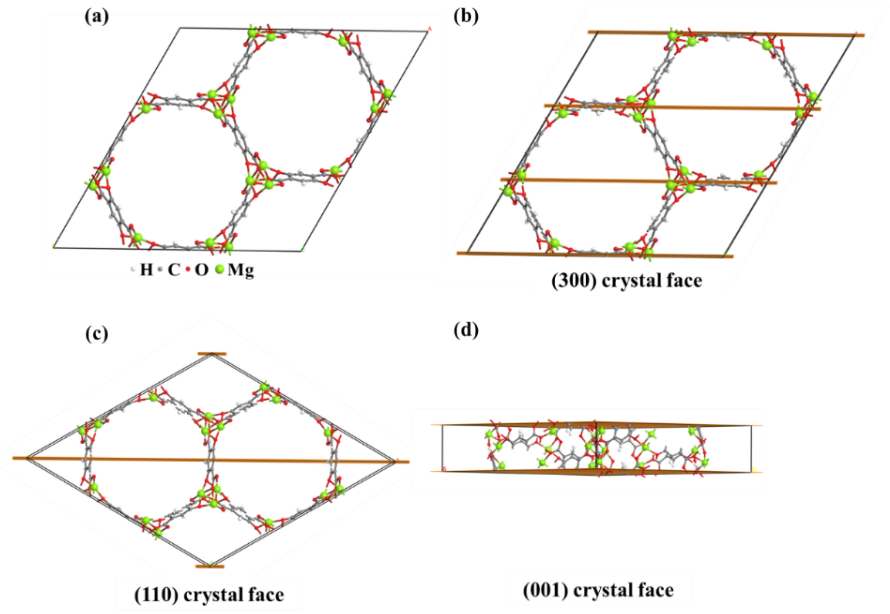

Figure S4. (a) Diagram of the Mg-MOF-74 cell structure. (b) (300) crystal face. (c) (100) crystal face. (d) (001) crystal face (Gray: C atom; Red: O atom; Green: Mg atom; White: H atom; Yellow horizontal line: crystal face)

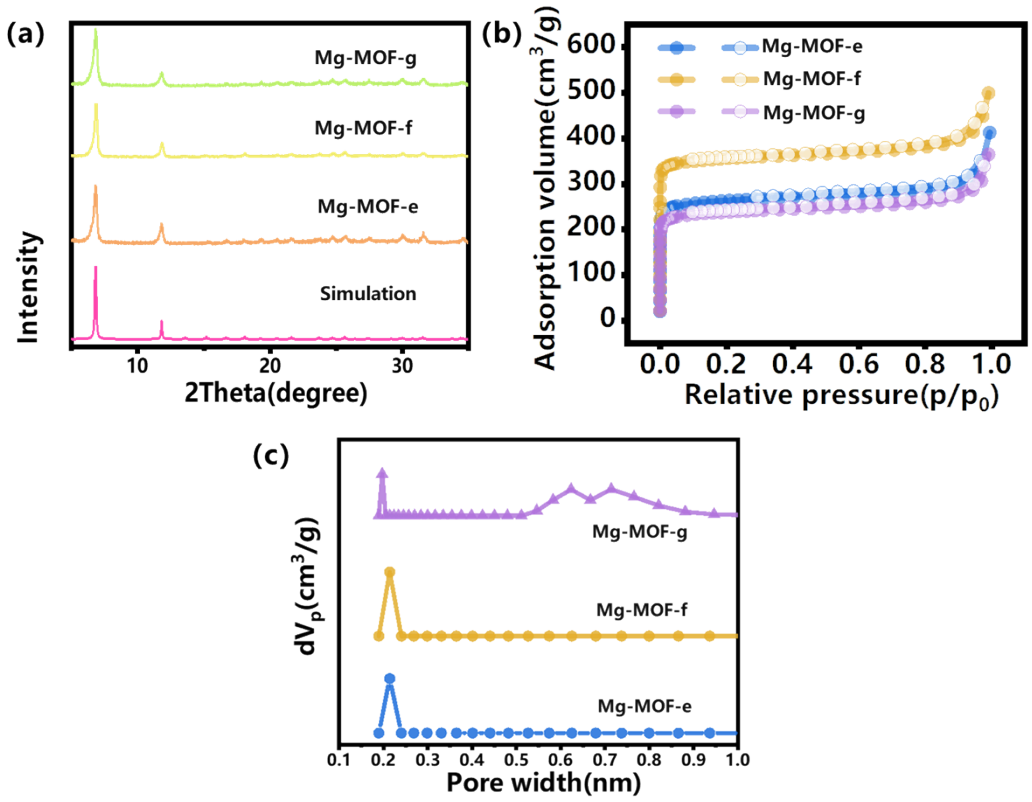

Figure S5. (a) XRD patterns, (b) BET specific surface area and (c) Pore volume of Mg-MOF-e-g synthesized with 1 mL, 1.5 mL and 2 mL deionized water additions, respectively.

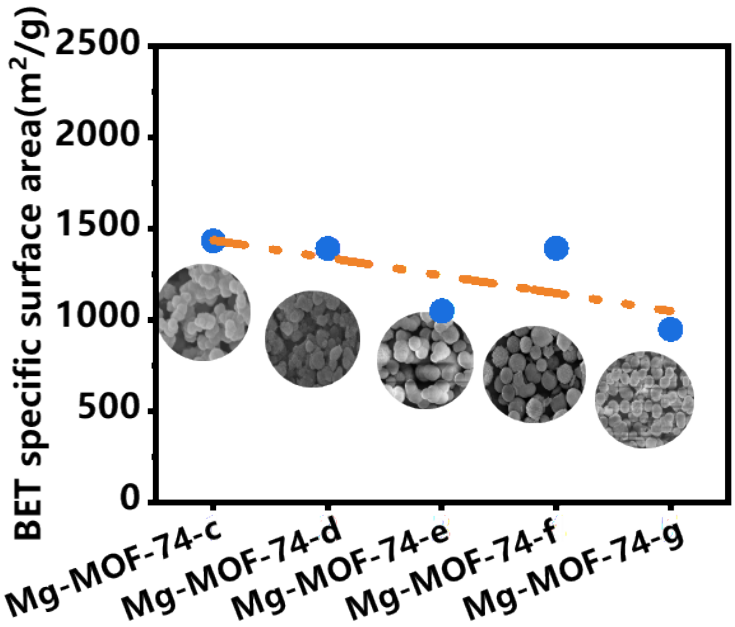

Figure S6. Variation of specific surface area with amount added water (c to g) from 0 mL to 2mL and the fitting curve is shown as the orange dashed line.

4.2 Synthetic modulation of Amines-Mg-MOF-74 materials.

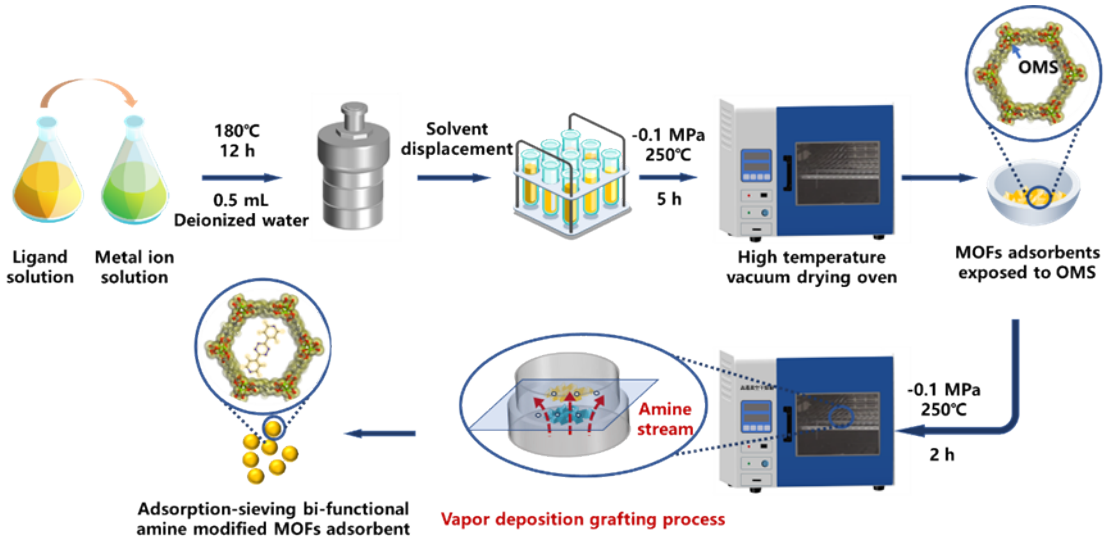

Figure S7. Schematic of the synthesized amine-modified Mg-MOFs process

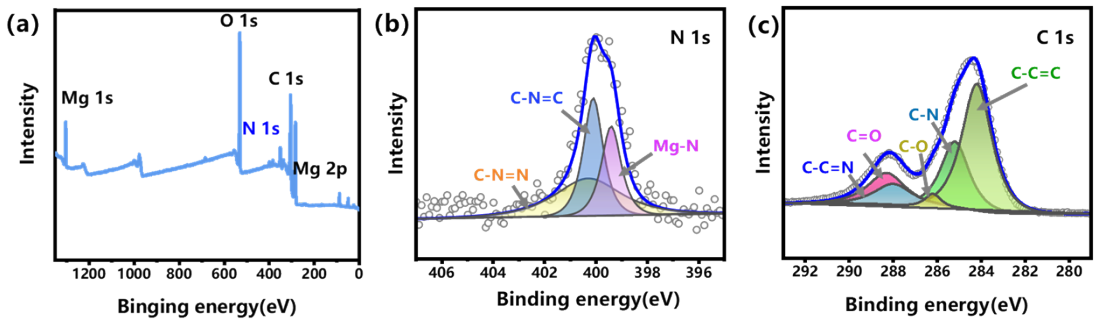

Figure S8. (a) XPS elemental analysis, (b) N-1s analysis and (c) C-1s analysis of MOF-amine-b, respectively.

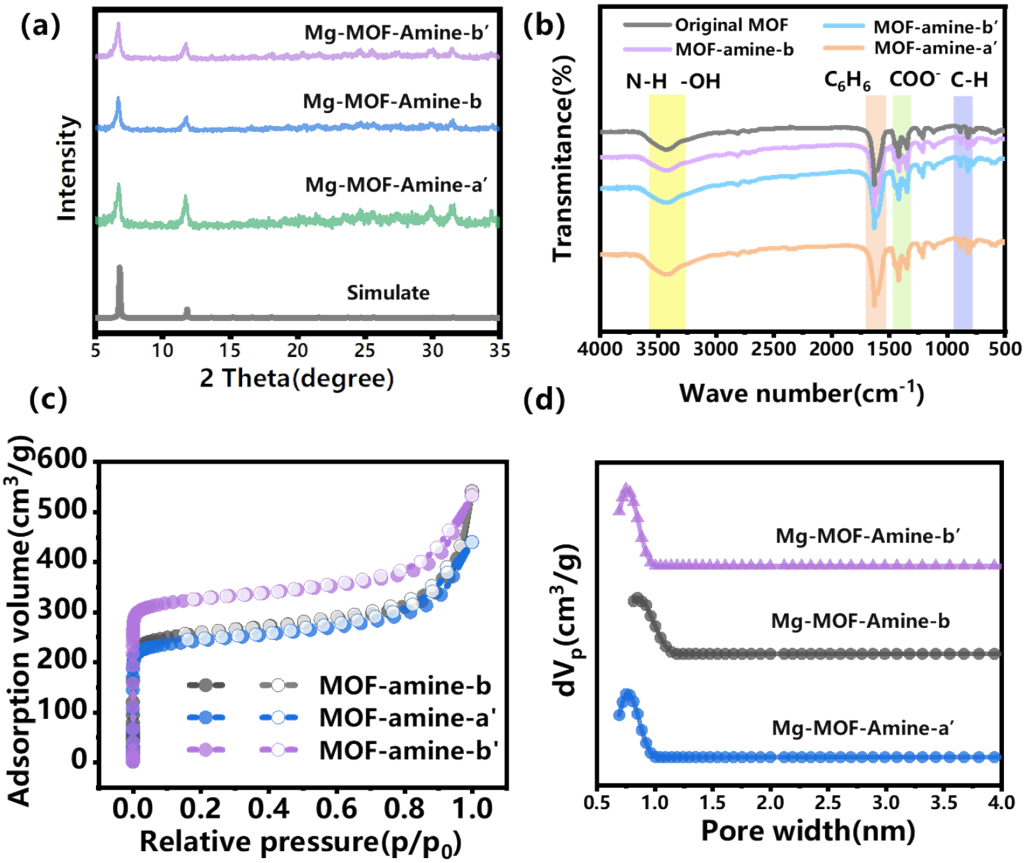

Figure S9. (a) XRD patterns of MOF-amine-a' and MOF-amine-b/b', respectively. (b) FTIR analysis. (c) BET specific surface area. (d) Pore volume, respectively.

4.3 CO_2 capture capacity and selectivity of Mg-MOFs and amine-Mg-MOF-74s materials.

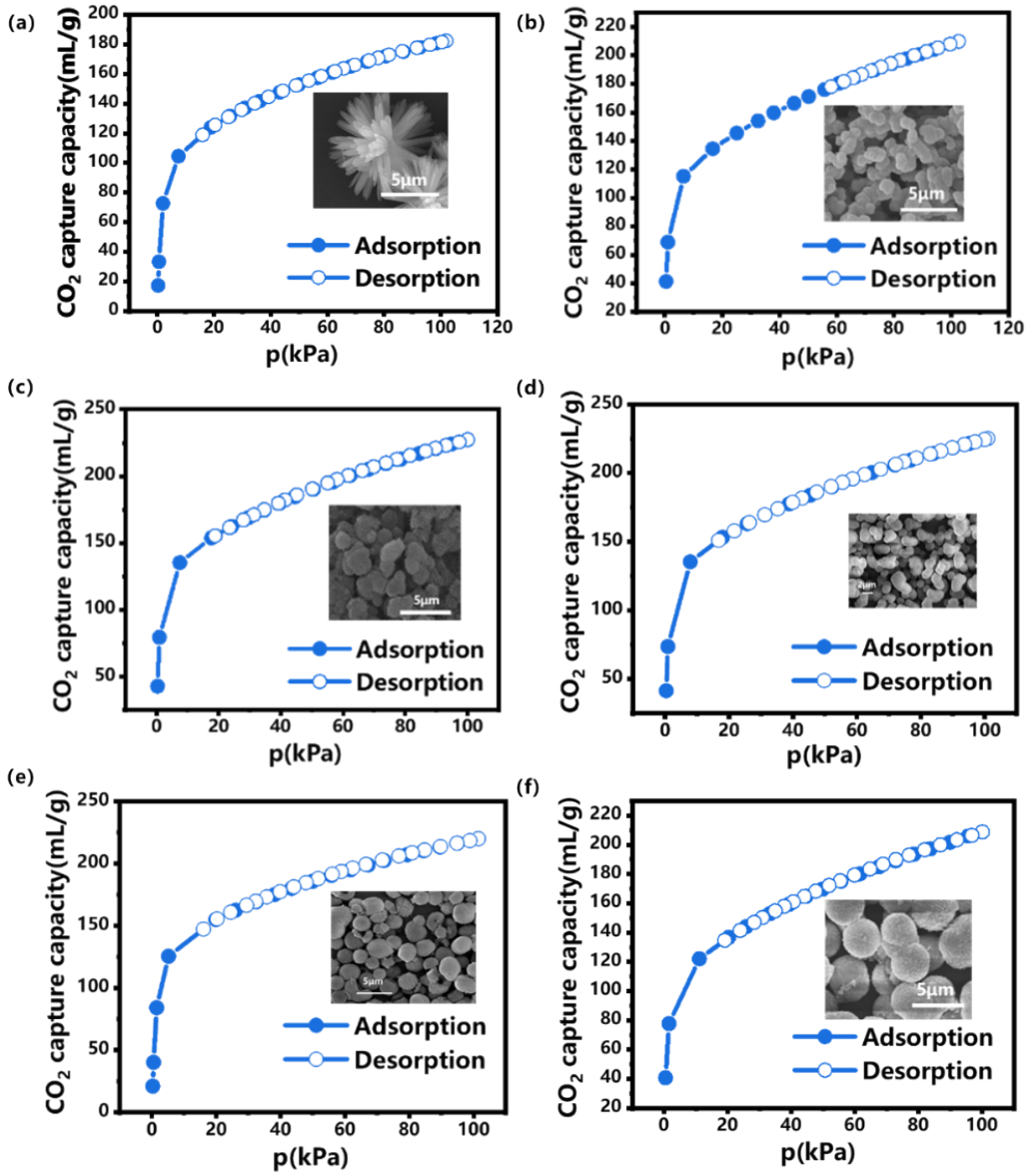

Figure S10. (a-f) CO_2 adsorption capacity curves for Mg-MOF-b-180 ℃, Mg-MOF-c-g at 273 K, respectively.

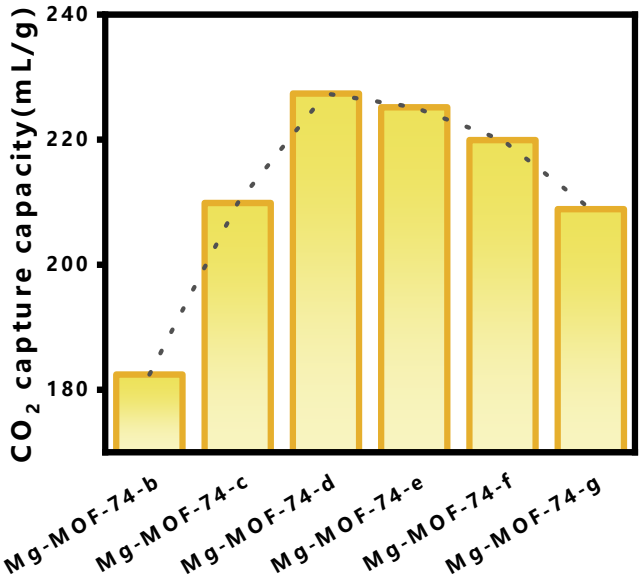

Figure S11. Maximum saturated adsorption capacity of CO_2 for Mg-MOF-b-g at 273 K, 1 bar.

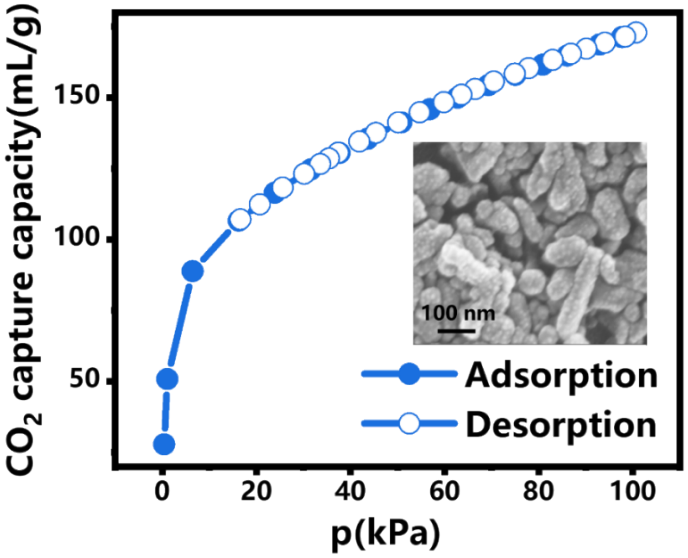

Figure S12. Maximum saturated adsorption capacity of CO_2 for Mg-MOF synthesized by mixed solvent of ethanol/DMF at 273 K, 1 bar.

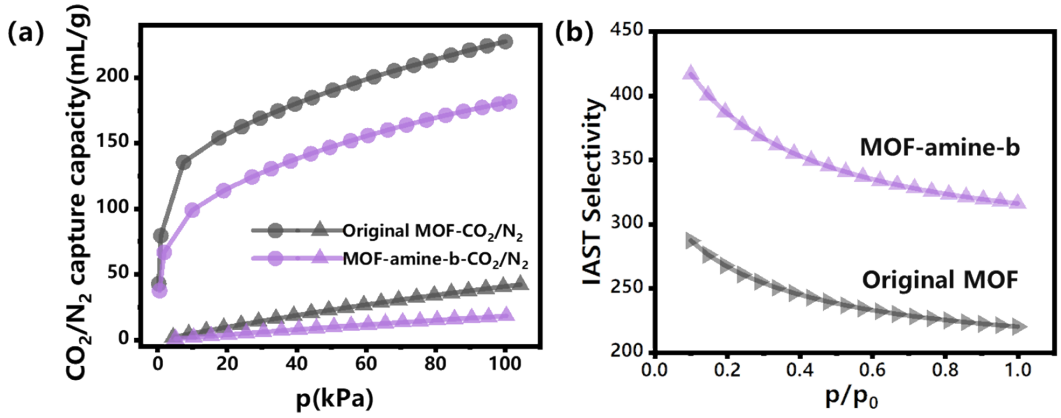

Figure S13. (a) CO_2 and N_2 adsorption capacity curves and (b) IAST selectivity for Mg-MOF and MOF-amine-b at 273 K, respectively.

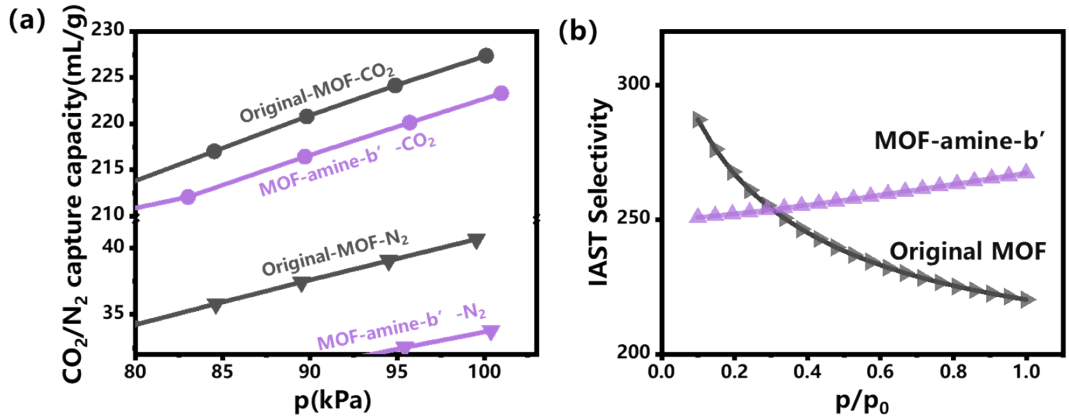

Figure S14. (a) CO_2 and N_2 adsorption capacity curves and (b) IAST selectivity for Mg-MOF and MOF-amine-b' at 273 K, respectively.

4.4 Molecular-level understanding of CO_2 adsorption and N_2 behavior.

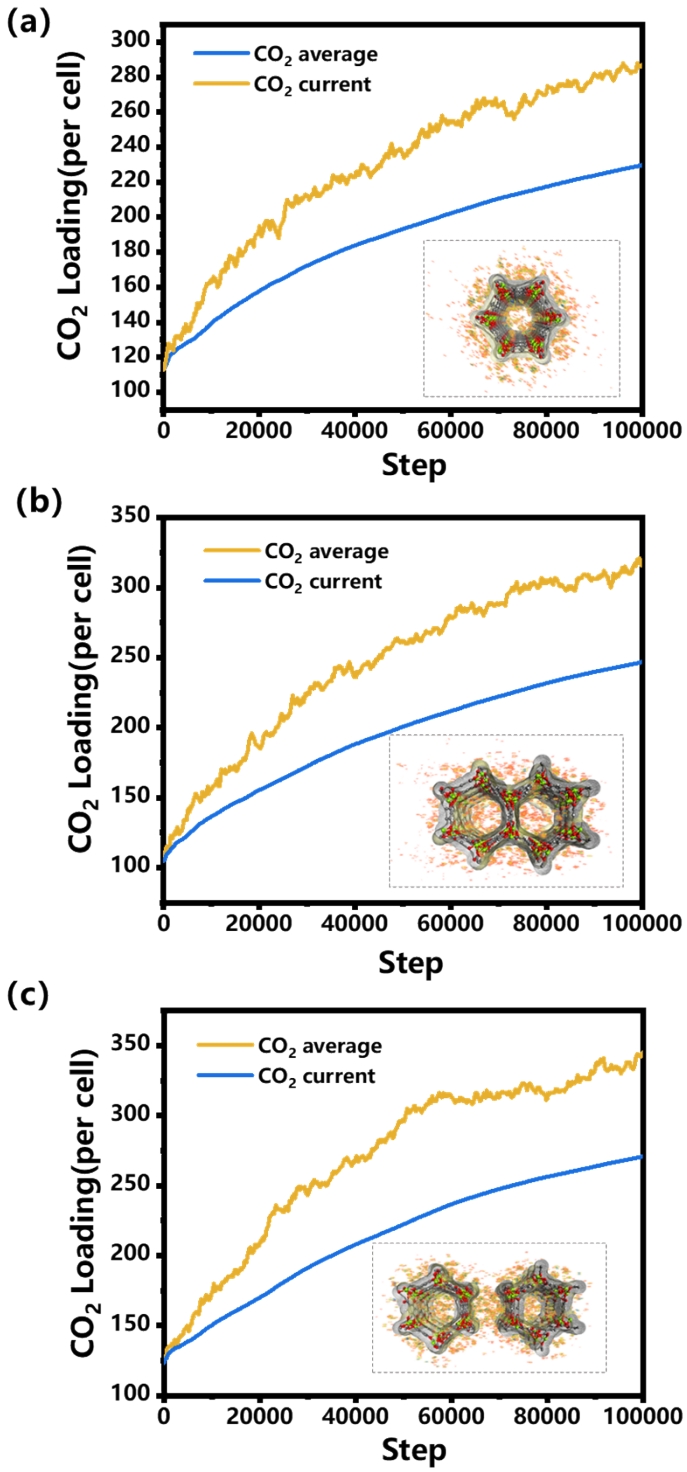

Figure S15. (a-c) CO_2 adsorption curve of cell 1-3 calculated by GCMC, respectively.

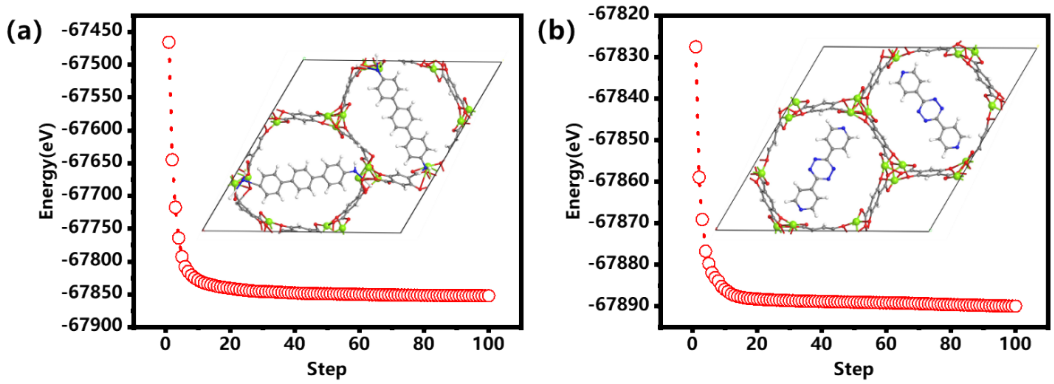

Figure S16. (a-b) Energy convergence for geometric optimization and structures of MOF-amine-a and MOF-amine-b after geometric optimization of DFT, respectively.

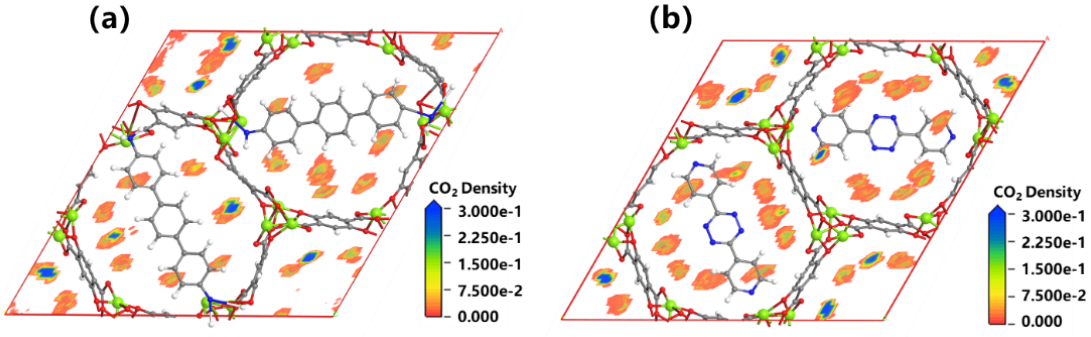

Figure S17. (a-b) CO_2 adsorption density of MOF-amine-a and MOF-amine-b calculated by GCMC.

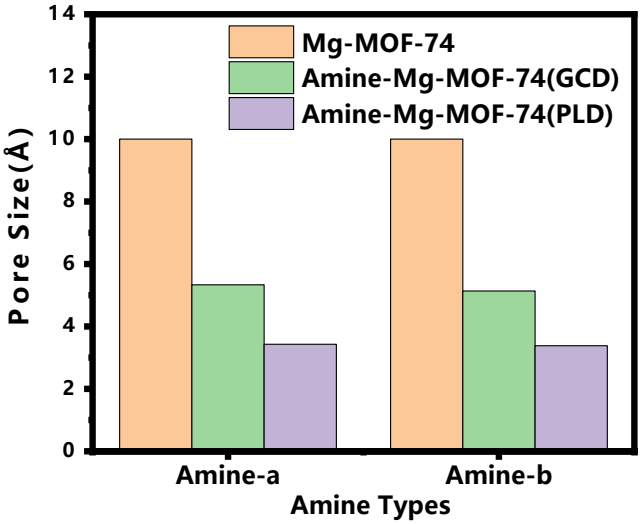

Figure S18. Pore size distributions (GCD and PLD) after amine-a and amine-b pore modification.

Table S1. Elemental analysis of MOF-amine-a and MOF-amine-b

Sample	C(wt%)	O(wt%)	Mg(wt%)	N(wt%)
MOF-amine-a	59.33	33.12	5.44	2.02
MOF-amine-b	58.59	33.40	5.78	2.23

Table S2. Comparisons of the maximum adsorption capacity and IAST adsorption selectivity(15% CO_2/85% N_2) of Mg-MOF-d, MOF-amine-a', MOF-amine-a at 273 K,1bar with other MOF-74 structures of the same series

Sample	Maximum adsorption capacity(mmol/g)	IAST adsorption selectivity	Ref.
Mg-MOF-d	10.13	221	This work
MOF-amine-a'	10	254	This work
MOF-amine-a	9.06	304	This work
Ni-MOF-74	8.29	50	[10]
Ni-MOF-74	7.48	32	[11]
Ni-MOF-74@Gro	5.76	45	[12]
HKUST-1	6.85	103	[13]
2GrO@HKUST-1	9.02	186	
Mg-MOF-74	9.37	138	[14]
M74@P	9.13	288	

5. Reference.

1. M. Díaz-García, A. Mayoral, I. Diaz and M. Sanchez-Sanchez, *Crystal growth & design*, 2014, **14**, 2479-2487.
2. P. Iacomi and P. L. Llewellyn, *Adsorption*, 2019, **25**, 1533-1542.
3. X. Tang, N. Ripepi, N. P. Stadie, L. Yu and M. R. Hall, *Fuel*, 2016, **185**, 10-17.
4. A. Kapoor, J. Ritter and R. T. Yang, *Langmuir*, 1990, **6**, 660-664.

5. S. E. Henkelis, S. M. Vornholt, D. B. Cordes, A. M. Slawin, P. S. Wheatley and R. E. Morris, *CrystEngComm*, 2019, **21**, 1857-1861.
6. Z. Meng and K. A. Mirica, *Nano Research*, 2021, **14**, 369-375.
7. P. Canepa, C. A. Arter, E. M. Conwill, D. H. Johnson, B. A. Shoemaker, K. Z. Soliman and T. Thonhauser, *Journal of Materials Chemistry A*, 2013, **1**, 13597-13604.
8. T. F. Willems, C. H. Rycroft, M. Kazi, J. C. Meza and M. Haranczyk, *Microporous and Mesoporous Materials*, 2012, **149**, 134-141.
9. R. L. Martin and M. Haranczyk, *Crystal growth & design*, 2014, **14**, 2431-2440.
10. L. Lei, Y. Cheng, C. Chen, M. Kosari, Z. Jiang and C. He, *Journal of Colloid and Interface Science*, 2022, **612**, 132-145.
11. C. Chen, X. Feng, Q. Zhu, R. Dong, R. Yang, Y. Cheng and C. He, *Inorganic chemistry*, 2019, **58**, 2717-2728.
12. T. Ghanbari, M. F. A. Patah, Y. H. Wong, F. Abnisa and W. M. A. W. Daud, *Fuel*, 2024, **372**, 131837.
13. F. Xu, Y. Yu, J. Yan, Q. Xia, H. Wang, J. Li and Z. Li, *Chemical engineering journal*, 2016, **303**, 231-237.
14. M. M. Jin, Y. X. Li, C. Gu, X. Q. Liu and L. B. Sun, *AIChE Journal*, 2020, **66**, e16645.